Spring 2024

Characterization of RNA Binding Proteins Regulating Axonal Localization of Prenyl-Cdc42 mRNA

Ashley I. Loomis
University of South Carolina

Director of Thesis: Dr. Jeff Twiss
Second Reader: Lauren Vaughn

Table of Contents

Thesis Summary

This project seeks to identify the mechanism for axonal localization of *prenyl-Ccd42* mRNA. There are two isoforms of *Cdc42* mRNA; *prenyl-Cdc42* localizes into the axons of neurons, while *palm-Cdc42* mRNA localizes into dendrites. CDC42 protein plays an important role in developmental and regenerative axon growth. This project aims to identify the region(s) of *Cdc42* mRNA responsible for driving this transcript into axons. Furthermore, we identify proteins that bind to *prenyl-Cdc42* mRNA proximal 3'UTR and are essential for its axonal localization. Knowledge gained from this study will increase understanding of axonal localization of mRNAs, as well as provide knowledge that can be used in future studies to find regeneration-promoting treatments for nervous system injuries. Understanding the mechanism(s) underlying spontaneous axon regeneration, including the functions of proteins like CDC42, is crucial for finding new approaches to promote successful nerve repair and restore neural function following traumatic injuries to the nervous system.

Introduction

1. Abstract

Following traumatic injury, axons in the peripheral nervous system (PNS) can spontaneously regenerate, albeit rather slowly. This regeneration requires messenger RNA (mRNA)-localization into and translation within the axons. One such mRNA originates from the *CDC42* gene, which produces two mRNA splice variants: Prenyl-CDC42 and Palm-CDC42 encoding mRNAs. CDC42 promotes axon growth and regeneration by regulating actin filament polymerization in growth cones of axons. This plays an important role to support nerve regeneration in humans. The *prenyl-Cdc42* mRNA is found in both central nervous system (CNS) and PNS axons, where it can be locally translated into CDC42 protein, which is subsequently prenylated. In this study, we identified that *prenyl-Cdc42* mRNA's axonal localization is dependent on a short motif within the 3' untranslated region (UTR), corresponding to nucleotides (nt) 764-800. RNA affinity mass spectrometry (RAMS) using biotinylated synthetic oligonucleotides corresponding to localizing 764-825 and non-localizing 800-875 nt sequences were used as bait to isolate and identify RNA binding proteins for these regions. RNA affinity pulldowns were performed using the localization sequence as bait with PC12 cell lysates to initially validate candidates identified by RAMS. This was later performed using lysates from cultures of dorsal root ganglion (DRG) neurons. The resulting bound fraction was analyzed by western blotting and probing for the specific RNA binding protein targets CCAR1, PTBP3, and MBNL1. CCAR1 and PTBP3 were validated as binding to the *prenyl-Cdc42* 764-825 nt (and later 764-800 nt). To further test for interaction between the localization motif on *prenyl-Cdc42* mRNA with CCAR1 and PTBP3, fluorescence in situ hybridization and immunofluorescence (FISH/IF) was performed using rat DRG neurons. CCAR1 colocalized with *prenyl-Cdc42*

mRNA in axons. siRNA knockdown of CCAR1, but not PTBP3, significantly decreased axonal signal for *prenyl-Cdc42* mRNA in DRG axons compared to a non-targeting siRNA. Together, these data indicate that CCAR1 is necessary for axonal localization of *prenyl-Cdc42* mRNA and provides new strategies for promoting axonal mRNA localization/translation and accelerating axon regeneration.

2. Background

2.1 Neurons

2.1.1 The nervous system

The nervous system is divided into two main categories: the central and peripheral nervous systems. The central nervous system (CNS) consists of the brain and spinal cord, while the peripheral nervous system (PNS) includes all the other neurons and nerves in the body (excepting cranial nerves I and II). The PNS has bundles of axons called ‘nerves’ coming from groups of neuronal cell bodies in the CNS or PNS. The PNS can be further divided into the somatic and autonomic nervous systems. The somatic nervous system is consciously controlled and consists of afferent and efferent neurons. Afferent PNS neurons recognize stimuli from their environments and relay this information to the CNS. Efferent neurons then carry this information away to either periphery effector cells (e.g., muscle) or other neurons. The autonomic nervous system is not consciously controlled and consists of the sympathetic and parasympathetic nervous systems. The sympathetic nervous system causes a stress response, and the parasympathetic nervous system relaxes the body.

2.1.2 Neuronal structure

Neurons consist of a cell body, dendrites, axon(s), and axon terminals. The soma, or cell body, of the neuron houses many of the cell's organelles, including the nucleus (Figure 2.1B). The dendrites receive signals in the form of neurotransmitters that bind to receptors on the cell surface. The summation of these signals can then produce an action potential that propagates to

the distal axon, relaying information from one end of the neuron to the other. Axons can be either myelinated or unmyelinated (Debanne et al., 2011). Myelin sheaths increase conduction rates of a nerve impulse, allowing the action potential of the neuron to flow down the axon faster. Action potentials are generated once the neuron receives enough excitatory signaling to reach a voltage threshold point. The neuron depolarizes, which occurs as the membrane potential becomes more positive, and then eventually repolarizes to its negative resting potential. The action potential is propagated along the entire length of the axon, jumping from node to node if the axon is myelinated through to the axon terminal. As the action potential reaches the axon terminal, a series of mechanism occur including the binding of calcium to the synaptotagmin protein, which interacts with SNARE proteins allowing vesicles to fuse to the membrane of the axon terminals and release the neurotransmitters via exocytosis into a small gap, the synaptic cleft, in between the two neurons (Figure 2.1A; Chapman, 2008). Neurotransmitters diffuse through the small area to bind to receptors on the next neuron's dendrites or target tissues, to either excite or inhibit the target (Figure 2.1A)

Most importantly for this project, the structure of the axons is fundamentally unique to the other cytoplasmic projections of the neuron. This difference is established during neuronal differentiation and specification. The neuron begins as a cell body with multiple short neurites projecting from the soma; eventually, one neurite has significantly faster growth and is established as the axon (Polleux & Snider, 2010). As axons serve different functions from the cell body and dendrites, they therefore have distinct features and are established as functionally distinct domains. Taylor et al. (2013) demonstrate that the morphology and microtubules of the axon establish this domain as fundamentally distinct from the rest of the neuron, with many functions being carried out by the axon that have little involvement from the cell body. Due to

the cytoskeleton of microtubules in the axon, unidirectional cell polarization is established, causing very controlled localization within the axon, unlike within the dendrites which have mixed microtubule polarization (Figure 2.1B) (Minc et al., 2009).

In this project, primary dorsal root ganglion (DRG) neurons are used as a peripheral neuron model and have a different structure from most other multipolar neurons (Figure 2.1C). DRGs are a cluster of cell bodies of neurons that also contain support cells, like satellite glia and Schwann cells. DRG neurons are 'pseudo-unipolar' and only extend axons not dendrites. In this case, the axon branches as a T-junction in these sensory neurons that receive signals (the peripherally projecting axon) and propagates signals to the CNS (the centrally projecting axon).

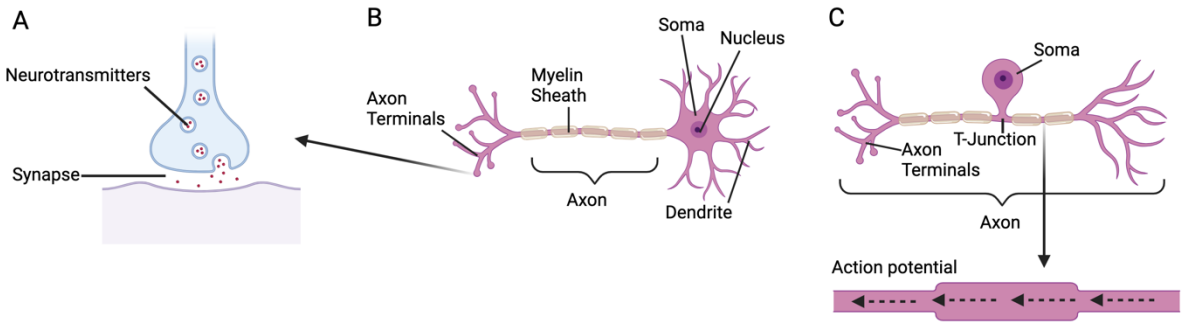

Figure 2.1: Neuronal Structure. (A) Neurotransmitters are then released into the synapse, the space between two neurons or between neuron and effector cell. A multipolar neuron (B) and pseudounipolar dorsal root ganglion neuron (C) are shown above. (B) Action potentials originate at the dendrites and travel along the myelinated axon until the axon terminals are reached. (C) The action potential in DRGs originate at the peripheral region of the axon and are carried toward the T-junction and continue down the axon in a unipolar, unidirectional manner until the axon terminals are reached.

2.1.3 Glial components of the nervous system

There are many other cells of the nervous system besides neurons. In the CNS, there are a particular set of glial cells: astrocytes, ependymal cells, and oligodendrocytes. Astrocytes provide nutrients to the neurons and synaptic regulation. Ependymal cells produce the cerebrospinal fluid that protects the brain and spinal cord. Oligodendrocytes provide the myelin sheath to the axons by wrapping cytoplasmic extensions around the axon many times that condense to form myelin. The PNS contains two types of glial cells: are the satellite cells or satellite glia and Schwann cells. The satellite cells function in protection, by activating and reentering the cell cycle to create new cells to replace the damaged one after injury (Chen et al., 2020). Schwann cells function similarly to oligodendrocytes in providing the myelin sheath to PNS axons and after injury they play a role in axonal regrowth. Another category of CNS cells are microglia, but these derive from the immune rather than nervous system embryologically and serve as macrophages to phagocytize dead cells, pathogens, and other debris. The PNS does not contain microglia and is not as immune privileged as the CNS.

2.1.4 Dorsal Root Ganglia & Sciatic Nerve

DRGs are found bilaterally alongside the spinal cord at each vertebra (Ahimsadasan et al., 2014). They contain groups of cell bodies of sensory neurons that function in sensing pain, temperature, touch, and proprioception. The axon bundles, or nerves, of these sensory neurons relay sensory information to their corresponding DRG, which houses up to 15,000 somas (Ahimsadasan et al., 2014). The peripherally projecting DRG axons are responsible for relaying sensory information to the soma, while the centrally projecting DRG axons enters the spinal cord

and synapse with interneurons in the spinal cord grey matter or the brainstem (Ahimsadasan et al., 2014).

The sciatic nerve runs from the lumbar and sacral regions of the spinal cord to the pelvis and down the entire leg into the foot. It is the largest nerve in the human body and innervates the skin and muscles of the leg and foot (Giuffre et al., 2023). Consequently, sciatic nerve carries motor information to the entire region of the leg and foot and sensory information from these regions back to the spinal cord. It contains both myelinated (motor, mechanosensing, and propriosensing) and unmyelinated (pain and temperature sensing) axons. In rats, the sciatic nerve functions very similarly and has a similar structure, also originating from the lumbar region of the spinal cord and running the length of their legs (Rigaud et al., 2008).

2.2 Messenger RNA synthesis & Processing

Now that the large-scale anatomy and physiology of the nervous system has been examined, the molecular processes occurring within these systems must be discussed. mRNA is a ribonucleic acid macromolecule that encodes proteins needed to give structure and function to all cells.

mRNA is used to carry the genetic information contained in nuclear DNA into the cytoplasm to be used as a template for synthesis of proteins. RNA is made of nucleotides, similar to DNA, but uses bases adenine (A), uracil (U), guanine (G), and cytosine (C) (instead of A, thymine (T), G, and C). When initially transcribed, RNAs contain both introns (non-coding regions), and exons (coding and 5’ and 3’ untranslated regions). mRNAs are transcribed by RNA polymerase II, which results in specific processing of the immature mRNA. mRNAs have directionality and run from their 5’ end to their 3’ end, like DNA. This directionality is utilized

when being read during translation. Processing includes splicing out introns as well as adding the 5’ cap and 3’ poly-A tail. The 3’ poly-A tails protect the mRNA from degradation and helps to promote translation (Passmore & Coller, 2022). The 5’ methylated "cap" also protects the RNA from promotes translation of mRNAs by being recognized by translation initiation factors (Galloway et al., 2019). Splicing can produce distinct mRNA isoforms from a single gene through alternative splicing of the pre-mRNA (Lee & Rio, 2015). For example, SR and hnRNP proteins work together to either enhance or silence, respectively, generating RNA isoforms that contain or exclude exons, oftentimes generating distinct protein isoforms (Figure 2.2) (Lee & Rio, 2015). For the focus of this thesis, *Cdc42* mRNA has two spliced isoforms that are determined by the differential expression of the splicing factors PTBP1 and PTBP2. The alternatively spliced Cdc42 mRNA isoforms can give rise to Prenyl-CDC42 vs Palm-CDC42 proteins with unique C-termini and 3’ UTRs.

Coding regions of mature mRNA are flanked by untranslated regions (UTR). These are important non-coding regions of the mRNA that contribute to post-transcriptional gene regulation in response to cellular signals and environmental cues. The 3' untranslated region, found after the coding region, often plays a role in regulating localization, stability, and translation (Lytle et al., 2007). On the other hand, the 5'UTR recruits ribosome attachment to initiate translation and can affect translation efficiency (Leppek et al., 2018). Ultimately, mRNA's structure and localization play an important role in the regulation of cellular activities via controlling protein availability. The ability of mRNAs to carry out these functions is often mediated by RNA binding proteins (RBP).

Although this project focuses on axonal localization and protein synthesis, it is important to note the complexities that surround the production and steady state levels of mRNA. How

much mRNA is present in the cell is determined by the balance of its synthesis and decay rates. Trans-acting agents can determine the synthesis and decay of mRNAs. For example, transcription factor activity can increase or decrease the level of individual mRNAs, while microRNAs or RNA decay factors can stabilize or destabilize an individual mRNA.

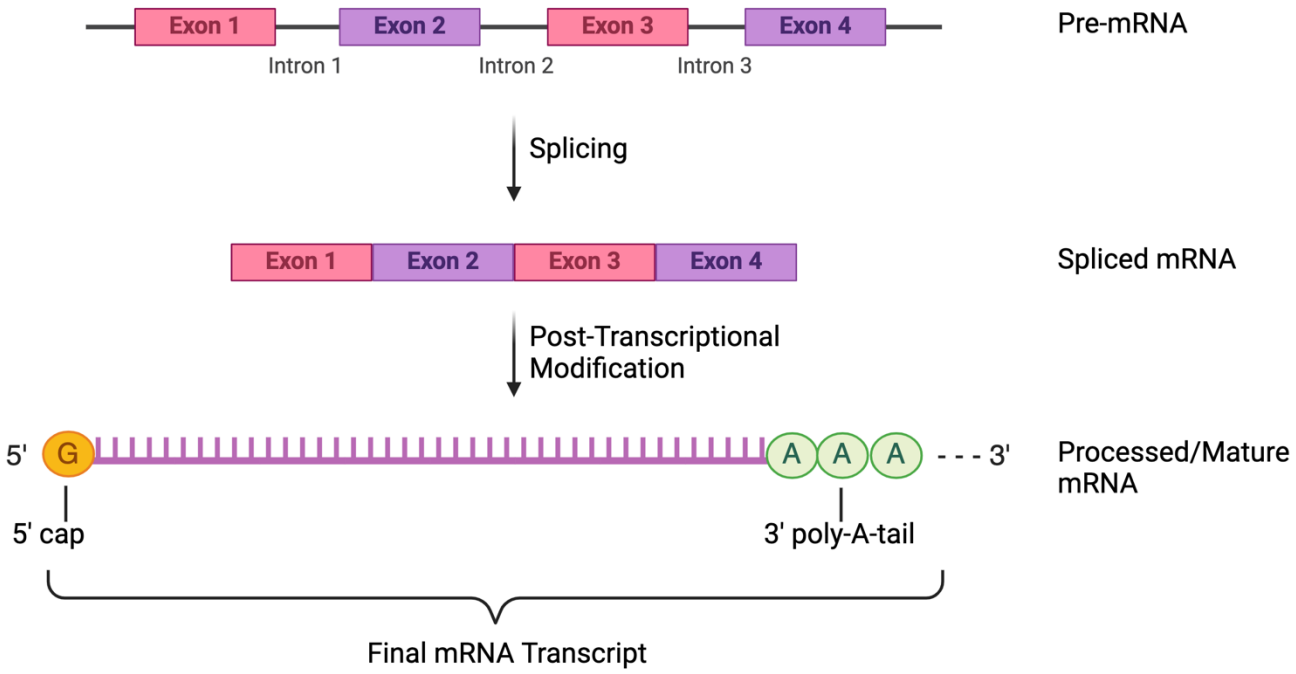

Figure 2.2: RNA processing. After transcription, but prior to modification, messenger RNA consists of exons and introns. During post-transcriptional modification, introns are spliced out of the mRNA transcript and exons are spliced together. The mRNA is given a guanine cap at the 5' end, and a poly-A tail at its 3' end.

2.3 Protein synthesis

The Central Dogma is a biological theory that states the flow of genetic information is unidirectional and goes from DNA to RNA to protein. We previously discussed the passing of information from DNA to mRNA and how mRNAs are processed and regulated.

Protein synthesis involves the translation of mRNA nucleotides into the building blocks of proteins called amino acids. Nucleotides are read in groups of 3 called codons with each codon specifying one amino acid. This is a universal genetic code, meaning the same codons code for the same amino acids in all species, though there is preferential usage of codons within different species. Translation requires the coordination of the mRNA, translation factors, the ribosome subunits, and charged transfer RNAs (tRNA).

Ribosomes contain a small (40S) and a large (60S) subunit both made of ribosomal RNA and proteins, that combine to form the complete 80S ribosomal complex. The ribosome carries out the synthetic aspects of translation as being the site of protein synthesis and facilitates reading of the genetic code by ensuring only proper codon-tRNA matches lead to amino acid addition to the growing peptide. tRNAs carry a designated amino acid on their 3' acceptor arm along with a separate loop structure containing an anticodon, which is largely complimentary to the codon on the mRNA. The tRNA pairing of the amino acid and anticodon provides the adaptor to move from nucleotide to amino acid sequence.

To begin translation, translation initiation factor elF4 binds to the 5’ cap on the mRNA and recruits other initiation factors that bind to the 40S ribosomal subunit. The 40S subunit and other translation factors then scan down the mRNA’s 5’ UTR until they reach the Kozak consensus sequence (Xie et al., 2023). Once this region is reached, the 60S subunit is recruited and the resulting 80S ribosome scans the mRNA for the start codon using the initiator tRNA anti-

codon. Once the start codon is identified, the large ribosomal subunit binds, and translation progresses by matching the anticodon of the tRNA to each consecutive codon of the mRNA. Amino acids are added one by one, and a polypeptide is formed. When finished the ribosomal complex disassembles and all components are recycled for use.

2.4 Axonal localization

For this project, it is important to look at protein synthesis through the lens of the axon. To better comprehend how axons utilize the polymerization of their cytoskeletons to tackle migration and growth, it is necessary to understand how, and which, proteins play roles in this mechanism. Hence, it is also crucial to recognize how proteins localize into the axon and the factors affecting this transition. Due to the length of the sciatic nerve and other axons, the localization across this distance is important for acute responses.

2.4.1 Localization sequences & RNA binding proteins

Localization sequences, or motifs, are usually found in the 3' untranslated region of the mRNA (Andreassi et al., 2018). Localization sequences are cis-elements in the RNAs that are recognized by RBPs (Li et al., 2021). Often, an RBP can recognize multiple motifs, so there is some promiscuity that is likely driven by secondary or tertiary structure rather than primary sequences (Gomes et al., 2014). A classic motif includes the AU-rich region (ARE) in the 3' untranslated region (Li et al., 2021).

RBP are proteins that are able to bind specific mRNA sequences and form ribonucleoprotein (RNP) complexes with the RNA. Protein composition within an RBP determines fate of the mRNAs, and can modulate its stability, subcellular localization, storage

or/and translation. One example of an RBP that promotes mRNA decay is KHSRP, which binds to AU-rich regions in the 3'UTRs of mRNAs and targets those mRNAs to cytoplasmic exosomes for degradation (Figure 2.3A) (Patel et al., 2022). In contrast, the RBP HuD similarly binds to AU-rich regions but promotes mRNA stability, localization, and translation.

RNPs that are used as transport granules have been shown to contain translational factors and ribosome units (Li et al, 2021). These RNP complexes can bind directly or indirectly to motor proteins on the cytoskeleton or to indirectly through vesicles associated with motor proteins (Corradi et al., 2018). For example, zipcode-binding protein 1 (ZBP1) binds to the 'zipcode' motif in the 3'UTR of beta-actin to carry the mRNA into the axons of neurons (Gomes et al., 2014). RBPs have been shown to associate with many different mRNAs, depending on the sequences or motifs within the sequence.

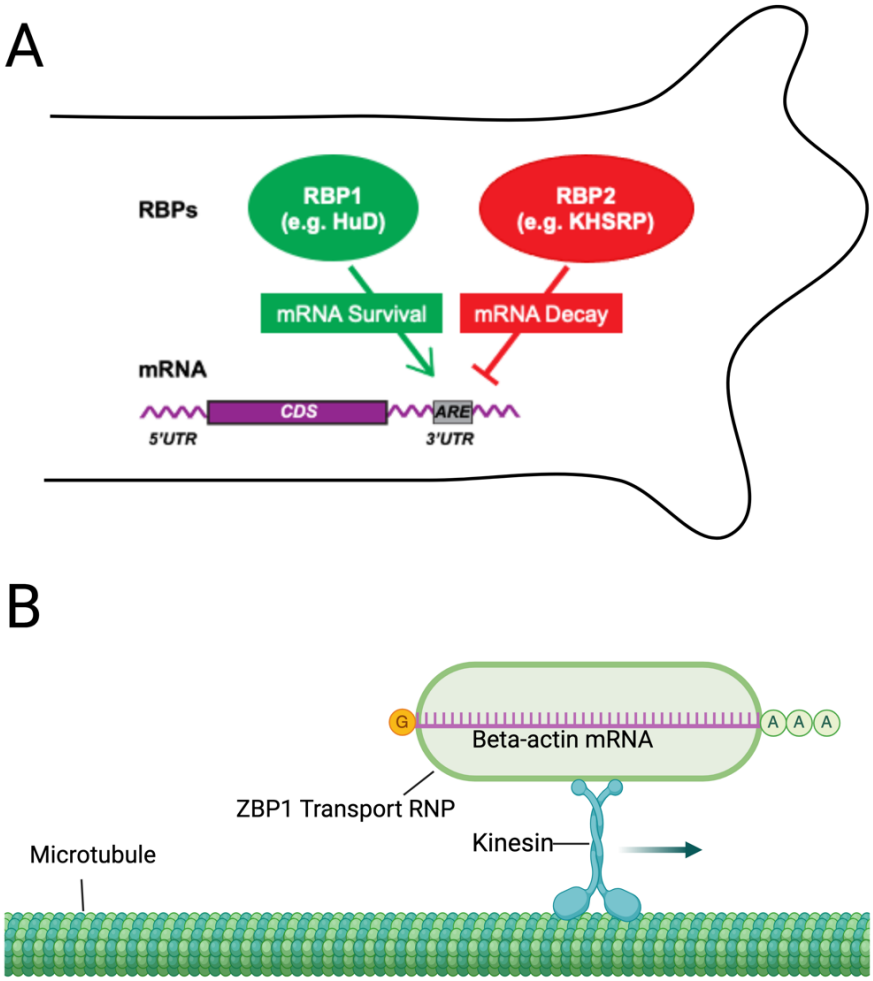

Figure 2.3: Functions of RNA binding proteins. (A) RBPs can either stabilize or destabilize mRNAs, affecting its translation into corresponding proteins. KHSRP is an example of an RBP that leads to mRNA decay, while HuD helps survival of mRNAs. (B) Another RBP is ZBP1 which binds to beta-actin mRNA and then to a kinesin protein that physically localizes the mRNA into the axons by utilizing motor function along the microtubule cytoskeleton of the axon. This shown helps to demonstrate the mechanism of localizing RBPs and how they function with mRNA strands.

2.4.2 Subcellularly localized protein synthesis

Although it was known that ribosomes localize into dendrites, it was only more recently that scientists have shown local protein synthesis occurs within axons as well. This was believed because there are polysomes, many ribosomes grouped together along with an mRNA typical of productive translation, present in the dendrites of hippocampal neurons but those same studies did not detect polysomes in the hippocampal axons (Torre & Steward, 1992). Despite the initial lack of polysomes, evidence of productive translation is found in axons of other neuron types (Piper & Holt, 2004). For local axonal protein synthesis to be accomplished, the neuron must transport mRNAs and translational machinery into the axonal compartment. The cell uses information from cis-elements in UTRs of mRNAs to decide which ones will be transported into the axon (Dalla Costa et al., 2021). RBPs binding to these motifs form an RNP and the newly formed RNP is transported as a membrane-less granule (Dalla Costa et al., 2021). While the mRNA is being transported, the granule seems to prevent translation of associated mRNAs until it reaches the appropriate point in the axon. Once the correct location is reached, the mRNA is released from the RNP or the RNP is remodeled to allow translation; however, some released mRNAs are held in stress granule-like compartments in axons until needed (Dalla Costa et al., 2021). With vesicle-based transport, the RNA binds to vesicles through an adapter protein(s) and release of the mRNAs occurs as outlined for RNPs in general above (Dalla Costa et al., 2021).

2.5 Model System--Nerve damage

2.5.1 Central nervous system damage

When damage or injury occurs in the CNS it is typically permanent. The mature CNS has low capability for regrowth after injury in adult mammals. More recently, scientists found that lack of regeneration is not only an intrinsic fault of these neurons, but also of the damaged environment around them unable to support regrowth (Benowitz et al., 2017). Benowitz et al. (2017) explain that glial scars are one of the greatest environmental barriers to axon regeneration in the CNS. Researchers Silver & Miller (2004) demonstrated that glial scars consist mostly of astrocytes and in the most severe cases, connective tissue elements. In response to injury, astrocytes increase in size and increase their production of intermediate filaments in order to stabilize tissues after damage, but this also decreases the ability for neurons to regenerate (Silver & Miller, 2004). Additionally, oligodendrocyte-derived proteins (from myelin) and astrocyte-derived proteins (proteoglycans) actively block axonal regeneration (Filbin, 2003).

2.5.2 Regeneration in peripheral nervous system

The PNS has a much greater ability to regrow after injury, in part due to the myelin-producing Schwann cells in the PNS instead of oligodendrocytes in the CNS. Schwann cells, assist in phagocytizing debris the degenerating nerve distal to an injury (Bhatheja & Field, 2006). Schwann cells also secrete laminin to form a basal lamina at their periphery. This is essentially a 'tube' that remains in place after injury and promotes the overall directionality of axon growth after injury (Bhatheja & Field, 2006). Schwann cells release neurotrophic factors like nerve growth factor to assist in regeneration and help to recruit pro-regenerative and -repair inflammatory cells to the nerve (Bhatheja & Field, 2006).

Unfortunately, across different mammalian species the rate of PNS axon regeneration is about 1-4 mm per day, and that rate decreases with increasing age (Höke & Brushart, 2009).

Thus, regenerative axon growth over long distances required in humans often time fails and can bring non-specific target reinnervation. This is partially due to the Schwann cells reverting to a non-supportive phenotype and the extracellular matrix undergoing changes that no longer support axon growth (Höke, 2006). Additionally, for axons that do make it to their targets, the targets are often no longer receptive for reinnervation. Consequently, the further an axon has to grow at 1-4 mm/day, the less likely it will be able to successfully regenerate to its target (Höke, 2006). Turkman et al. (2023) found that surgical repair of this injured nerves in humans also results in a poor outcome if the distance is more than 5 cm, with variable to completely lacking recovery of motor and sensory function. This highlights that regeneration rate is a limiting factor for functional recovery, so methods to accelerate PNS regeneration are desperately needed and some of those methods are likely to be applicable for CNS regeneration.

2.6 CDC42

Research is ongoing to better understand sciatic nerve injury and various mechanistic pathways that could be altered to enhance regeneration speed. CDC42 is a protein that affects growth and migration of the axon, and is upregulated following injury, hence the importance in studying this protein and its mRNA's regulation.

2.6.1 CDC42 protein

CDC42 is a small Rho GTPase well known to regulate cytoskeletal dynamics. CDC42 binds and hydrolyzes the nucleotide triphosphate GTP causing the protein to cycle between an inactive (GDP bound) state and an active (GTP bound) state that is able to bind to downstream effectors (Etienne-Manneville & Hall, 2002). CDC42 plays roles in apoptosis, cell cycle

regulation, and growth through regulating cytoskeleton organization (Kalpachidou et al., 2021). CDC42 also functions in axon growth and cell motility by assembling filopodia and actin microspikes (Figure 2.4) (Lee et al., 2018). Interestingly, CDC42 can promote both actin polymerization and depolymerization in axonal growth cones (Kalpachidou et al., 2021). CDC42 is produced in developing and adult DRGs and as mentioned previously, has an increased expression following PNS damage (Kalpachidou et al., 2021). Since CDC42 largely influences axon growth and is upregulated post injury, we sought to understand how this protein is produced & maintained locally in the axons during regeneration.

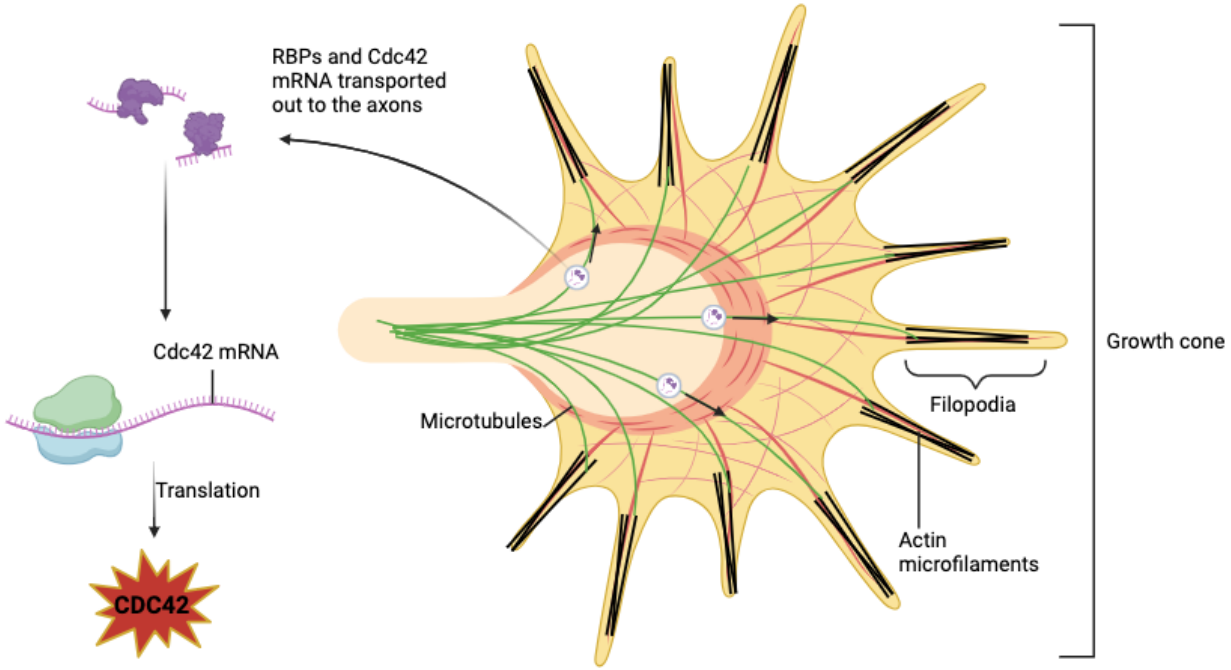

Figure 2.4: Local translation of CDC42. Local translation of CDC42. Localization of RNP complex of Cdc42 to the growth cone of an axon. Vesicles containing RNP complex travel down microtubules. CDC42 promotes the organization of actin microfilaments and growth of filopodia.

2.6.2 Differential localization of CDC42

Alternative-spliced isoforms of *Cdc42* mRNA give rise to the Palm-CDC42 and Palm-CDC42 proteins. The palmitoylated CDC42 protein isoform contains a C-terminal CCaX motif that is post-translationally modified by palmitoylation (Lee et al., 2021). This protein is encoded by a *Cdc42* mRNA isoform that contains exons 1 though 6 (Figure 2.5). The prenylated CDC42 protein contains a C-termina CaaX motif that is post-translationally modified by prenylation. This protein is encoded by a *Cdc42* mRNA containing exons 1 through 5 and exon 7 (skipping exon 6; Figure 2.5). *Palm-Cdc42* mRNA only localizes into dendrites while the *prenyl-Cdc42* mRNA localizes into dendrites and axons (Figure 2.4; Lee et al., 2021). The differential utilization of exon 6 and 7 in these two mRNA splice variants leads to mRNAs with different 3'UTRs, which are responsible for their subcellular localization (Lee et al., 2021). My thesis project focuses on the *prenyl-Cdc42* mRNA 3'UTR motif(s) that are responsible for its axonal localization.

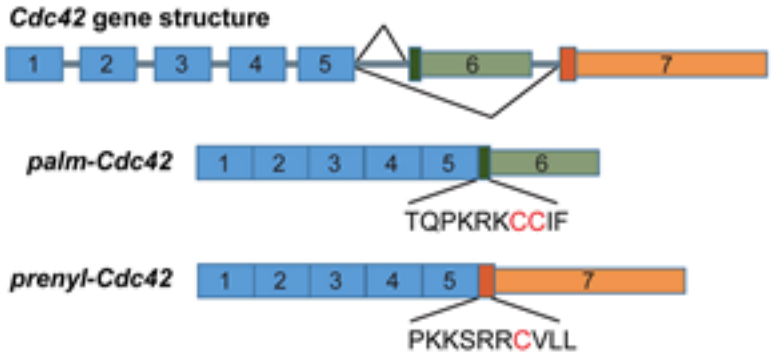

Figure 2.5: CDC42 isoforms. *Cdc42* nuclear RNA initially has 7 exons prior to post-transcriptional splicing. It is alternatively spliced to contain exons 1-6 or exons 1-5 plus exon 7

(i.e., skipping exon 6). The former results in the palmitoylated version of CDC42 and the latter is the prenylated version of CDC42, which can localize into axons.

3. Methods/Methodologies

3.1 Cloning

3' UTRs of *prenyl-Cdc42* mRNA from various vertebrate species were compared using ClustalW (https://www.genome.jp/tools-bin/clustalw) to find highly conserved regions. Nt 764-838, 801-875, and 839-913 of rat *prenyl-Cdc42* sequence were cloned into the 3' UTR of CaMKlla-myr-EGFP 3' gamma-actin, replacing the gamma-actin sequence. This plasmid vector contains the coding sequence (CDS) of myrEGFP, which encodes for the green fluorescent protein (GFP) with a mryistoylation element for co-translational modification.

First the inserts were amplified by polymerase chain reaction (PCR). The inserts and plasmid were cut with restriction enzymes NotI-HF and XhoI, and then fractionated on agarose gels, to purify the digested DNA sequences. The DNA was extracted using Qiaex Gel Extraction Kit (Qiagen). The inserts were ligated into the $eGFP^{MYR}$5' Camklla/3'Actg plasmid vector using T4 DNA ligase (NEB), which was then transformed into competent *E. coli.* Using GeneJET plasmid mini prep kit, the plasmid vectors were isolated from the bacteria and their concentration was determined via SpectraMax microplate reading. To verify the incorporation of each insert, the final products were digested with restriction enzyme HindIII then fractionated on a 3% agarose gel. DNA constructs with successful ligation were validated by Eton Biosciences.

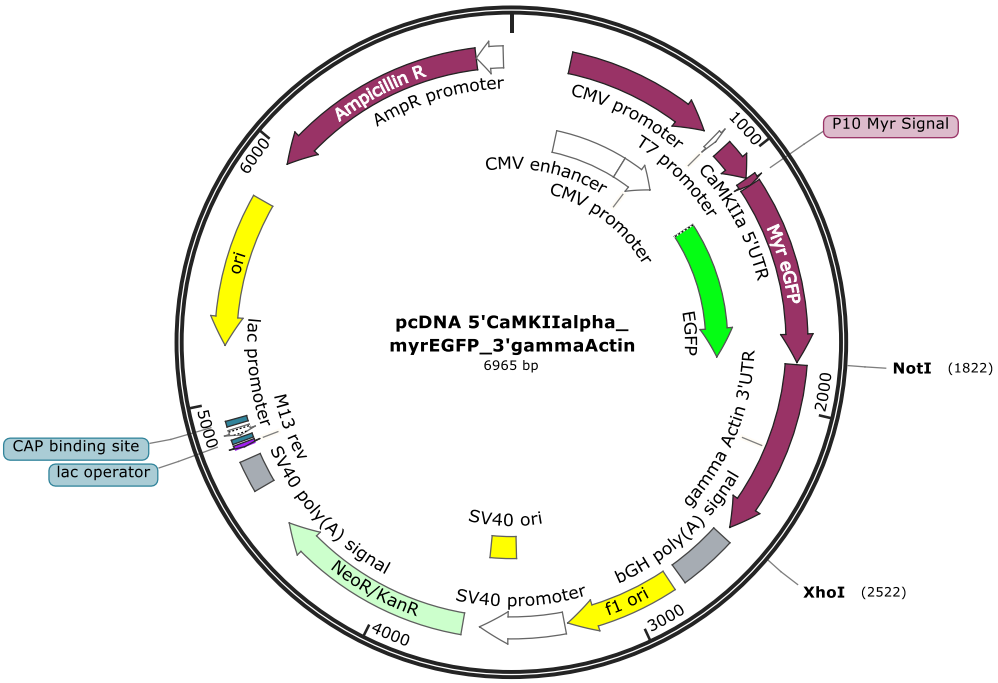

Figure 3.1: The eGFP^{MYR}5' Camklla/3'Actg vector. Backbone for cloning in 3' UTR deletion constructs. This was cleaved at nt 1822 and 2522 by restriction enzymes NotI-HF and XhoI and the gamma-actin piece excised. The *prenyl-Cdc42* 3'UTR segments were then ligated in downstream of the eGFP CDS, retaining the non-localizing 5'UTR of CamkIIa.

3.2 Animal use

All animal procedures used were approved by the Institutional Animal Care and Use Committees (IUCAC) of the University of South Carolina. DRGs were isolated from Sprague Dawley rats for DRG cultures for FISH/IF experiments. Rats were also used for cDNA in cloning (NCBI ID: XM_008764286 for prenyl-Cdc42; XM_008764287 for palm-Cdc42). All animals were euthanized by CO2 asphyxiation per IACUC guidelines.

3.2.1 Dorsal Root Ganglion harvest & culture

DRG cultures were performed as previously described (Twiss et al., 2000). Briefly, acid-etched glass coverslips coated with poly-L-lysine for 1 hour at 37˚C. Poly-L-lysine (Sigma) was removed and washed with sterile H2O. The plate was allowed to air dry and then 5 μg/mL laminin (Sigma-Millipore) in phosphate-buffered saline (PBS) was added and incubated overnight at 4˚C. The laminin was removed the next day and coverslips were washed with 1 x PenStrep in PBS. This was aspirated off and complete media (1X N1, 100 μM AraC, 10% Fetal bovine serum (FBS), 1x L-Glutamine, DMEM F12 50/50, and 1x Penicillin/Streptomycin) was added to each well and left at 37˚C while DRGs were harvested and dissociated (see below).

After euthanasia, DRGs were microdissected using a microscope. 8-10 DRGs were collected in 1.5 mL tubes each containing 1 mL of collection media (10 μL N1 and 990 μL Hiberate A). The DRGs were later transferred to 24-well plates and washed with complete media using microscissors to transfer ganglia between wells (which snipped the perineurium). Collagenase was added to 2000 units/mL [50 μL Collagenase in complete media per 10-12 DRGs] and the DRGs incubated at 37˚C for 15 minutes. The DRG suspension was triturated using a fire-polished glass pipette to break the ganglia apart. The DRGs were then transferred to a 15 mL conical tube and media was added to a total volume of 10 mL. DRGs were centrifuged at 0.1 x g for 10 minutes. The media was aspirated off and the pellet was resuspended in 10 mL of wash media and triturated 15-20 more times and centrifuged again. The wash media was aspirated off and the cell pellet was resuspended in complete media, and then plated in 24-well plates (approximately 0.5-2 DRGs per well). The wells were cultured overnight at 37˚C, and media was changed every 24-48 hours.

3.2.2 Sciatic nerve crush & harvest

Sciatic nerve crush was performed as described previously (Patel et al., 2022). Briefly, the rats used for sciatic nerve crushes were anesthetized with 5% isoflurane induction followed by 2% maintenance. The animals then received a sciatic nerve crush at mid-thigh level, approximately 2.5 cm from the nerve's origin with #2 fine jeweler's forceps, twice for 15 seconds each. The animals were monitored daily for well-being, noting that sciatic nerve crush prevented the animals from being able to use their hind limb. At 7 days following nerve injury, the animals were euthanized using CO_2 asphyxiation. The animals' sciatic nerves were then harvested, and 4-6 sciatic nerves were placed into each 1.5 mL tubes containing 200 µL of transfer buffer [10X PBS, water, protease inhibitor cocktail (PIC), and RNasin plus (Promega)].

3.3 RNA affinity mass spectrometry (RAMS)

Magnetic streptavidin beads (M280, Invitrogen) were equilibrated with buffer washes [0.1 mM NaOH, 50 mM NaCl] and Binding Buffers [2 M NaCl, 10 mM Tris (pH 7.4), 1 mM EDTA] to prepare the beads for oligo binding. RNase inhibitor and biotinylated synthetic RNA oligos were added to their respective beads and allowed to rotate at 4˚C for 30 minutes. The beads were then washed with CEB low salt [10 mM HEPES (pH 7.4), 3 mM $MgCl_2$, 14 mM NaCl, 1 mM DTT, 5% glycerol, H_2O].

Axoplasm was extracted from excised sciatic nerves by crushing the nerves by extrusion using a mini-pestle. The crushed sciatic nerves were spun down at 21,000 x g for 10-15 minutes at 4˚C. The supernatant was then added to the Streptavidin beads and rotated again at 4˚C for 30 minutes.

Beads were washed with binding buffers and CEB low salt. The lysate plus beads were then added to the binding beads with probes. After allowed to rotate at 4˚C for 30 minutes, they

were washed with high CEB salt and elution buffer (CEB high salt [10 mM HEPES (pH 7.4), 3 mM $MgCl_2$, 250 mM NaCl, 1 mM DTT, 5% glycerol, H_2O] and RNase) was added. The elutions were allowed to incubate at 37˚C for 15 minutes then spun down. The elute was transferred to low binding e-tubes. 4X SDS buffer with dye were added and an SDS page was ran. Each lane was cut into 10 individual pieces and stored at -80˚C until sent for mass spectrometry (MS) at UCSF Proteomics Facility. MS spectra were acquired between 375 and 1500 m/z with a resolution of 120000 FWHM. For each MS spectrum, multiply charged ions over the selected threshold (2E4) were selected for MS/MS in cycles of 3 seconds with an isolation window of 1.6 m/z.

3.4 PC12 cell culture

To collect preliminary validation data for the RAMS experiment, PC12 cell lysates were utilized. The PC12 cells were maintained in complete media (DMEM, 6% calf serum, 6% horse serum, and 1x Penicillin/Streptomycin) and used at less than 30 passages. For passing, the cells were centrifuged at 1000 x g, and the cell pellet was resuspended in 10 mL of media and plated on 10 cm plates. The cells would be split as needed to prevent overgrowth and cell death by removing the media in the plates and washing with 1X PBS.

3.5 RNA affinity immunoblotting

Immunoblots were used as preliminary validation of RAMS protein candidates. Samples from PC12 cells or rat axoplasm were prepared as above. Lysates were normalized for protein content by BCA assay (BioRad).

Pulldowns were fractionated on 10% SDS/PAGE gels prepared under RNAse-free conditions [DEPC H2O, Tris pH 8.8, Tris pH 6.8, 10% SDS, TEMED, Acrylamide, and 10% APS]. Followed by electrophoresis transfer to PVDF membranes. Membranes were blocked in Tris-buffered saline plus 0.5% Tween-20 (TBST) for 1 hour at room temperature followed by primary antibody diluted in the same blocking buffer overnight at 4˚C. The following primary antibodies were used: rabbit anti-CCAR1 (1:1000; Novus RBP1-86626), mouse anti-PTBP3 (1:1000; Santa Cruz sc-398105), mouse anti-MBNL1 (1:1000; Protein Tech 66837), and mouse anti-QK1 (1:1000; Abcam ab186245). After washing in TBST, blots were incubated in the following HRP-conjugated secondary antibodies at room temperature for 1 hour: anti-mouse IgG antibody (1:5000; Jackson ImmunoRes.) After extensive washing with TBST, immunocomplexes were detected by chemiluminescence using ECL (Amersham) and imaged using the ChemiDoc MP Imaging System (BioRad).

3.6 Fluorescence *in situ* hybridization (FISH) & immunofluorescence (IF) staining

siRNAs were utilized to deplete CCAR1 and PTBP3 in order to determine if depletion affected axonal *prenyl-Cdc42* mRNA levels. Stellaris probes were synthesized to bind to *prenyl-Cdc42* mRNA by FISH. CCAR1 and PTBP3 antibodies used for immunoblotting were also used for IF (1:200). Either chicken anti-NF (1:1,000, Aves labs) or SMI312 mouse anti-phospho-NF (1:500, Biolegend) were used as primary antibodies to mark neurons; visualization of GFP-tagged CDC42 proteins in growth cones utilized rabbit anti-GFP (1:500, Abcam). FITC-conjugated donkey anti-Rabbit (1:200, Jackson ImmunoResearch), FITC-conjugated donkey anti-chicken and donkey anti-mouse (1:200, Jackson ImmunoResearch), and/or Cy5-conjugated donkey anti-chicken (1:200, Jackson ImmunoResearch) were used as secondary antibodies.

Hybridization buffer consisted of 50 % dextran sulphate, 10 µg/ml E. coli tRNA, 10 mM ribonucleoside vanadyl complex, 80 µg BSA, and 10 % formamide in 2× SSC in a 15 mL tube. The hybridization buffer was then split into 20 500 µL aliquots (stored at -20˚C).

Coverslips from DRG cultures were washed with 1X PBS, fixed in 2% PFA, permeabilized in 0.3% Triton-X-100/PBS, and then equilibrated in hybridization buffer. The Stellaris probe, primary antibodies, and Roche 10X Blocking buffer were added directly into the Hybridization buffer at a 1:100 ratio. Coverslips were then inverted onto 30 µL of the probe/antibody mixture and put in a humidified chamber for 12-16 hours at 37˚C.

The secondary antibody was added into the hybridization buffer and Roche 10X Blocking buffer was added at a 1:100 ratio and mixed overnight at 4˚C. Coverslips from the previous day were washed with PBS + 0.3% Triton-X-100 and inverted onto secondary antibody mixture in humidified chamber. After 1 hour incubation in a humidified chamber sat at 37˚C, coverslips were washed with 1X PBS and mounted onto glass slides using ProLong (Thermo Fisher Scientific). After having sat at room temperature for 1 hour and 37˚C for an additional hour, the slides are imaged immediately.

3.7 Imaging, image analysis, & processing

High content imaging was used for neurite outgrowth analyses such that at least 15 neurons per coverslip were analyzed using a confocal microscope. Four channels were utilized: DAPI for nucleus staining, GFP for Neurofilament (NF), Cy3 for CCAR1, and Cy5 for PTBP3.

Using the ImageJ program, images were processed by extracting RNA signals from FISH probes within each optical plane that intersected with axonal markers (NF) on the xy plane (Terenzio et al., 2018). The intensities of mRNA signals across individual xy planes were

subsequently standardized according to the area of NF immunoreactivity (Kalinski et al., 2015). The average relative intensity of mRNA signals was calculated across all image locations within each biological replicate. Excel (Microsoft) software was used for statistical analyses.

4. Results

4.1 Identification of localization motif

The 3'UTR of *prenyl-Cdc42* mRNA was previously shown to drive axonal localization in neurons (Lee et al, 2020). Thus, we asked which distinct sequence within the 3'UTR was responsible for this. UTR sequences that are conserved across different species have been used to predict functional motifs in mRNAs. More than 85% of the first 150 nt of the proximal region of *prenyl-Cdc42* mRNA's 3' UTR (nt 764-913) was found to be conserved in 26 other vertebrate species using Clustal Omega multiple alignment tool (Sievers et al., 2011) (Figure 4.3). Thus, we asked if this highly conserved region is sufficiently responsible for axonal localization of a heterologous mRNA. For this, *prenyl-Cdc42* nt 764-913 or 914-2164 were cloned into the GFP reporter plasmid immediately downstream of the CDS. Stellaris FISH and IF imaging was used to visualize GFP mRNA in axons of cultured DRGs transfected with these GFP plasmids. *Prenyl-Cdc42* nt 764-913 was capable of localizing GFP mRNA into axons while nt 914-2164 was not (Figure 4.2 D). This indicated that *prenyl-Cdc42* mRNA localization motif resides within nt 764-913. We used deletion analysis of this region to determine if a shorter sequence might be sufficient for axonal localization by the same GFP reporter transfection assay. *Prenyl-Cdc42* mRNA's nt 764-838, 801-875, and 839-913 were then cloned as the 3'UTR for GFP. *eGFP^{myr}3'prenyl-Cdc42$^{764-838}$* showed axonal localization of the GFP mRNA, but the *eGFP^{myr}3'prenyl-Cdc42$^{801-875}$* and *eGFP^{myr}3'prenyl-Cdc42$^{839-913}$* showed no significant axonal GFP mRNA signals above control (Figure 4.2 E). Since eGFPmyr3'*prenyl-Cdc42*$^{801-875}$ showed non-significant axonal localization of eGFP mRNA, the overlapping 801-838 nt between the first and second insert was removed from the first insert to produce the sequence 764-800 nt. The

eGFPmyr3'*prenyl-Cdc42*$^{764\text{-}800}$ construct showed clear axonal localization of GFP mRNA (Figure 4.2 E). Together these data indicate that *prenyl-Cdc42* mRNA localizes through nt 764-800 in its most proximal 3'UTR.

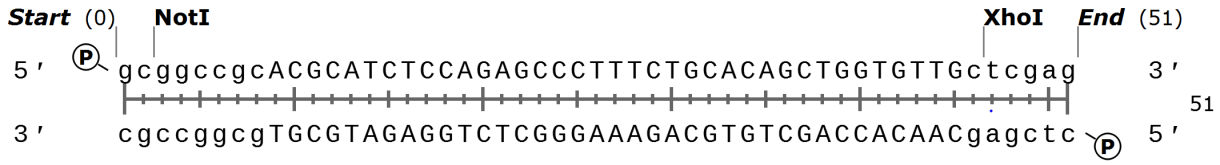

Figure 4.1: Localization motif nt 764-800 sequence. Sequence of insert used to create eGFP reporter construct utilizing nucleotides 764-800 of the Rat *prenyl-Cdc42* mRNA sequence as the 3'UTR.

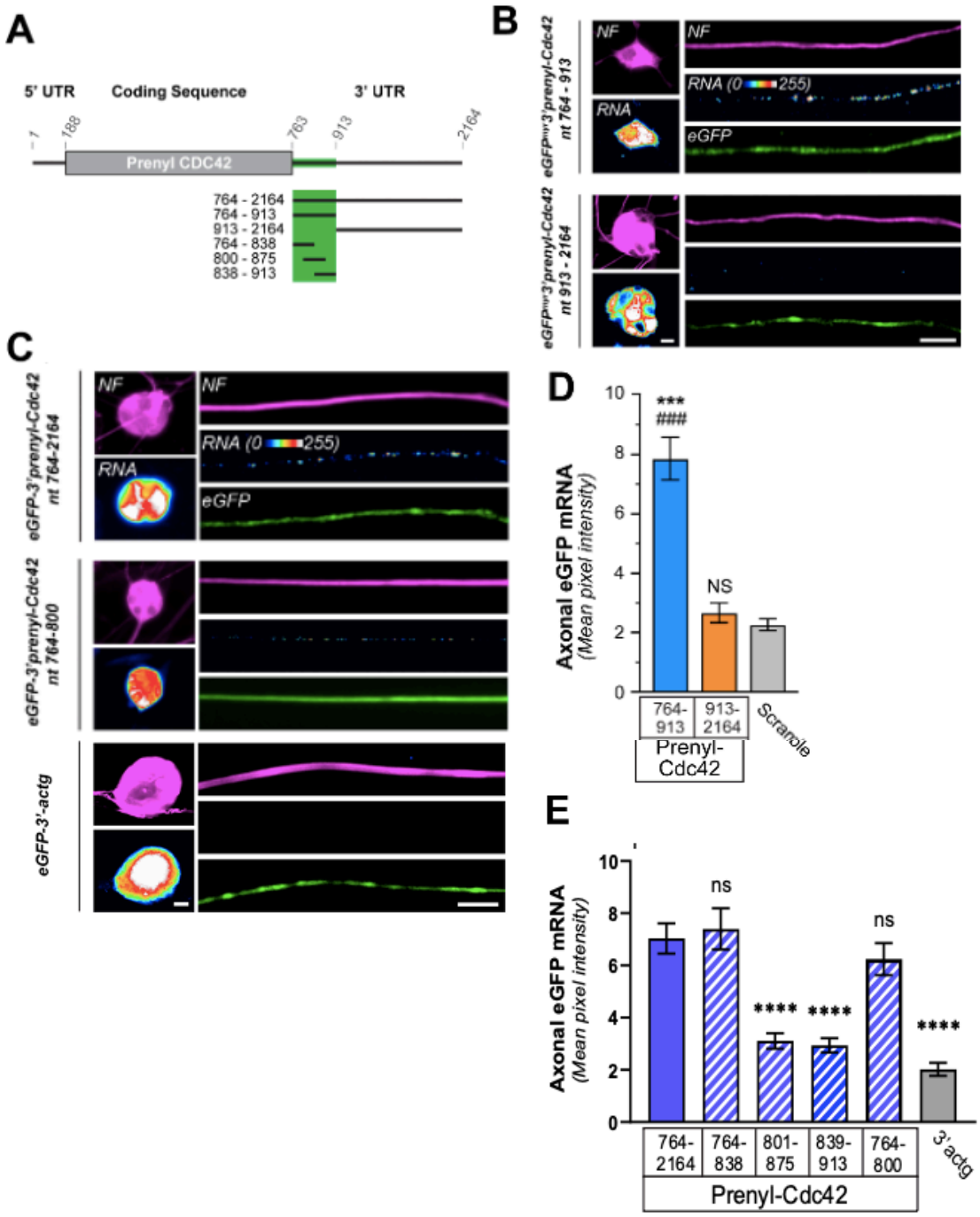

Figure 4.2: Nt 764-838 is sufficient for *prenyl-Cdc42* mRNA axonal localization. (A)

Schematic of the three insert sequences derived from sequence 764-913 within prenyl-Cdc42

mRNA's 3'UTR. (B) Stellaris FISH and IF images are shown for adult DRG neuron cultures transfected with eGFP^{myr}3'*prenyl-Cdc42*$^{764\text{-}913}$, or eGFP^{myr}3'*prenyl-Cdc42*$^{914\text{-}2164}$. Scale bars: 10 μm. (C) Stellaris FISH and IF images are shown for adult DRG neuron cultures transfected with GFP^{myr}3'*prenyl-Cdc42*$^{764\text{-}2164}$, eGFP^{myr}3'*prenyl-Cdc42*$^{764\text{-}838}$, eGFP^{myr}3'*prenyl-Cdc42*$^{801\text{-}875}$, eGFP^{myr}3'*prenyl-Cdc42*$^{839\text{-}913}$, eGFP^{myr}3'*prenyl-Cdc42*$^{764\text{-}800}$, and eGFP^{myr}3'*γ-actin*. Scale bar: 10 μm. (D) Quantification of FISH signals (from B) via pixel intensity above the background intensity. ***P<0.005 compared to 913-2164, ###P<0.005 compared to scramble (one-way ANOVA with pair-wise comparison with Tukey post-hoc tests). (E) Quantification of FISH signals (from C) via pixel intensity above the background intensity. Further deletion analyses indicate that nt 764-800 contains the axonal localization motif and mRNAs not containing this region do not show axonal localization above the control eGFP^{MYR}3'Actg. ****P<0.001 compared to 764-838, #### P<0.001 compared to 764-2164 (one-way ANOVA with pair-wise comparison with Tukey post-hoc tests).

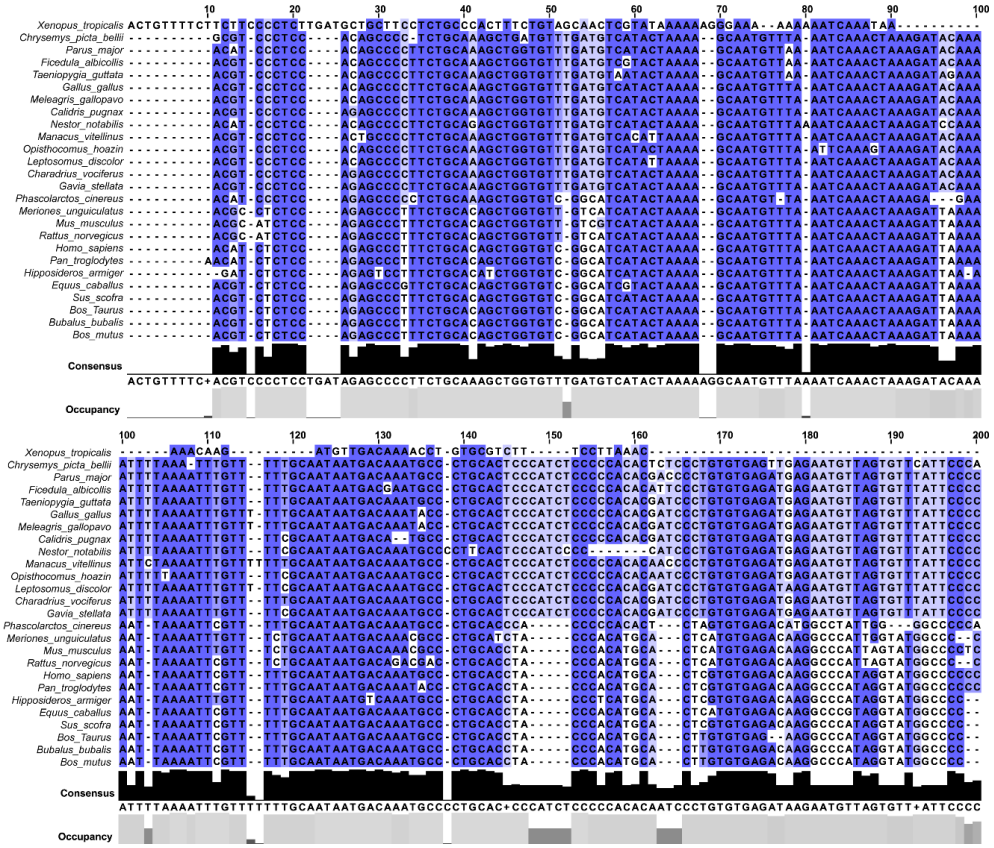

Figure 4.3: The proximal region of *prenyl-Cdc42* mRNA's 3' UTR is conserved in mammalian species. Clustal Omega alignments for *prenyl-Cdc42* mRNA's 3'UTR are shown for various mammalian species. The region 764-913 nt within the 3'UTR of *prenyl-Cdc42*'s mRNA show ≥85% conservation within mammalian species. The blue shading shows which bases are conserved across different species.

4.2 RAMS for *prenyl-Cdc42* RNA binding protein candidates

We next asked what axonal RNA binding proteins can bind to *prenyl-Cdc42*'s 3'UTR localization motif. RAMS was utilized to initially uncover binding proteins using sciatic nerve axoplasm. Biotinylated synthetic RNA oligonucleotides for nt 764-838, 801-875, and a scrambled control were utilized as bait for RAMS. MS measured the mass-to-charge ratio of proteins present in the axoplasm pulldown sample of *prenyl-Cdc42* mRNA. Previous studies

from our lab indicated that proteins showing above the 1.5-fold enrichment and with greater than $P \geq 0.05$ significance could potentially be RNA binding proteins for the RNA motif. The known RNA binding proteins CCAR1, PTBP3, and MBNL1 showed highly enriched binding to nt 764-825 of *prenyl-Cdc42* mRNA but not to nt 801-875. Notably, other RBPs showed lower but still significant binding to nt 764-825 (hnRNPK, hnRNPII, CCAR2, CPSF3, and CSTF2) and RBPs QK1, Elavl1, RBMS2 and COPZ2 showed enriched binding to nt 801-875.

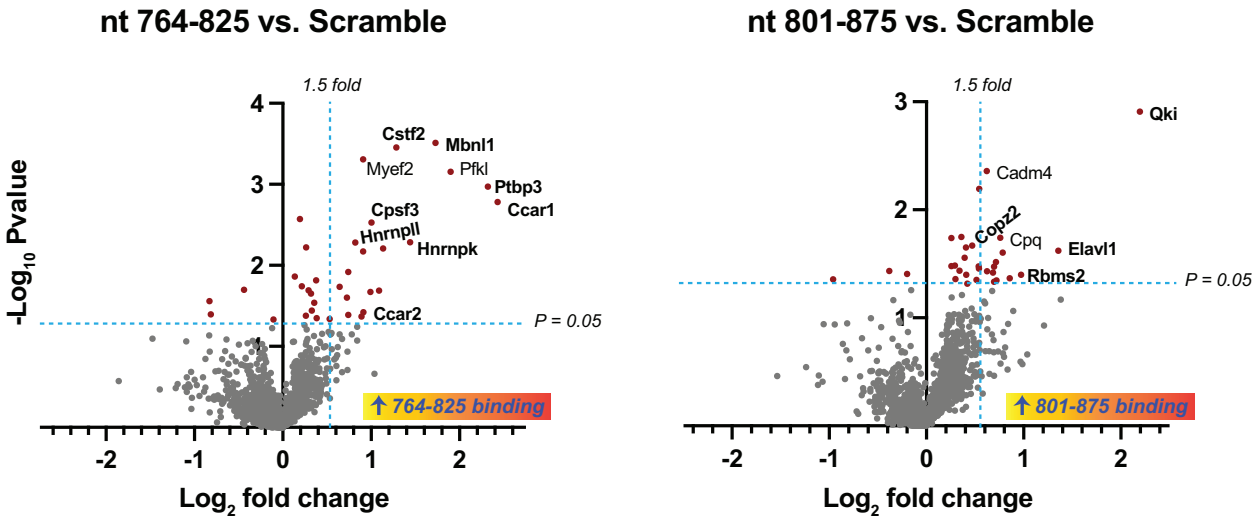

Figure 4.4: Many potential proteins may be necessary RNA binding proteins for *prenyl-Cdc42*. Mass spectrometry results from RAMS assay analysis is shown as volcano plots for IPs using nt 764-838 (left) and nt 801-875 (right) as bait vs. compared to scrambled oligonucleotide for each. Possible interacting RBPs were determined as above 1.5-fold change and below p=0.05.

4.3 Validation of CCAR1/PTBP3/*prenyl-Cdc42* mRNA interaction

To validate MS data, we analyzed RNA affinity pulldowns using immunoblotting to visualize specific proteins associated with *prenyl-cdc42* 3'UTR segment 764-800 nt. Both

CCAR1 and PTBP3 coprecipitated with the biotinylated oligonucleotide corresponding to nt 764-800 but not the scrambled oligonucleotide (Figure 4.5). Antibodies for MBNL1 showed multiple bands in the input, none of which corresponded to the predicted molecular weight, and no signals in the oligonucleotide pulldowns (Figure 4.5). QK1 similarly showed no binding to the 3'UTR motif; note this was anticipated, as the RAMS assay showed QK1 binding to nt 801-875 rather than not 764-838 nt (Figure 4.5).

These results above indicate that CCAR1 and PTBP3 can bind to sequences in the localization motif of *prenyl-Cdc42* mRNA, but these did not address the functional significance of this interaction. To address functionality, we used siRNA knock down of CCAR1 or PTBP3 and asked if this affected axonal levels of endogenous *prenyl-Cdc42* mRNA in axons using FISH/IF. siRNA knockdowns for CCAR1 in DRG cultures showed significantly decreased axonal signal for *prenyl-Cdc42* mRNA in DRG axons compared to the non-targeting siRNA (Figure 4.6). This was not the case for PTBP3 knockdown where axonal *prenyl-Cdc42* levels were comparable to non-targeting siRNAs.

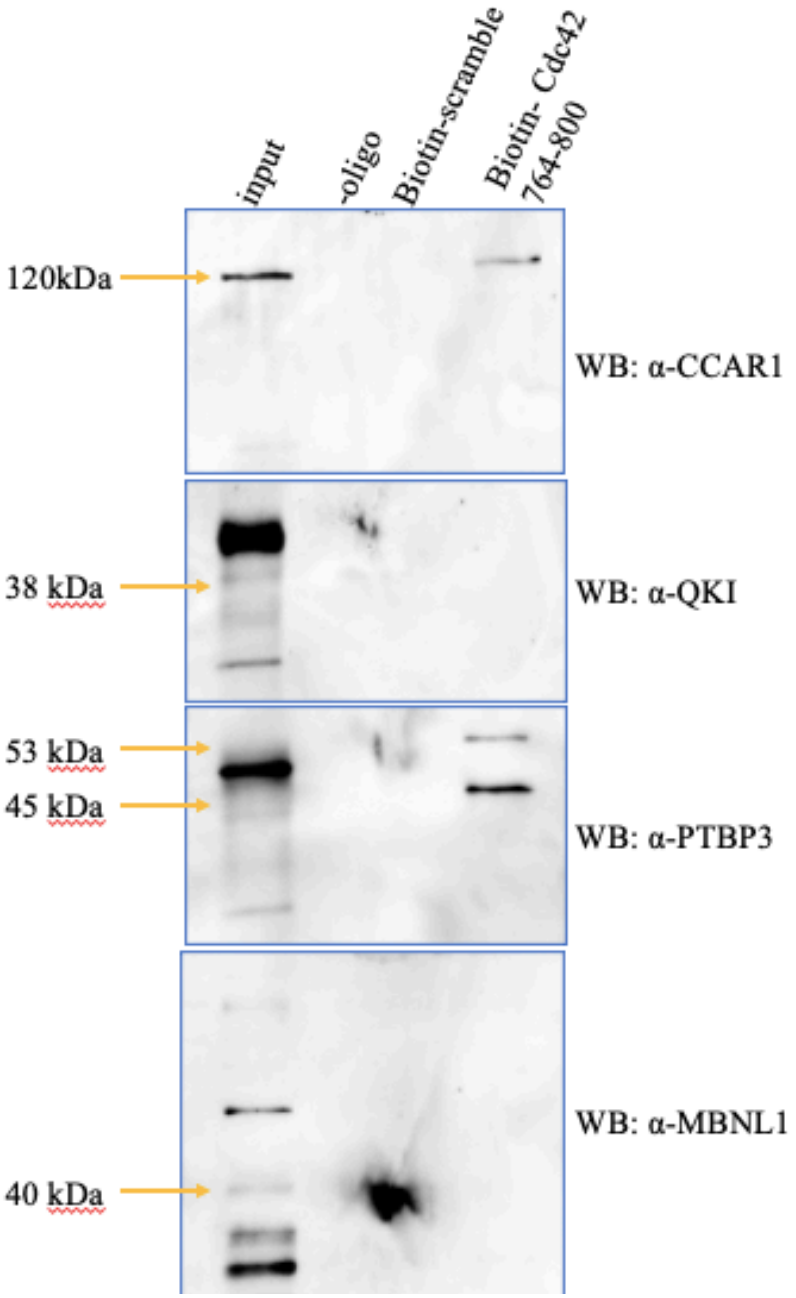

Figure 4.5: CCAR1 and PTBP3 associate with *prenyl-Cdc42* mRNA's 3' UTR localization motif. RNA affinity western blot is shown. Sample with no oligo, Biotin-scramble, and Biotin containing *prenyl-Cdc42* 3'UTR sequence 764-800 nt were ran on the western blot. Antibodies anti-CCAR1, anti-PTBP3, anti-QK1, and anti-MBNL1 were utilized with bands appearing in consistency with expected band size for CCAR1 and PTBP3.

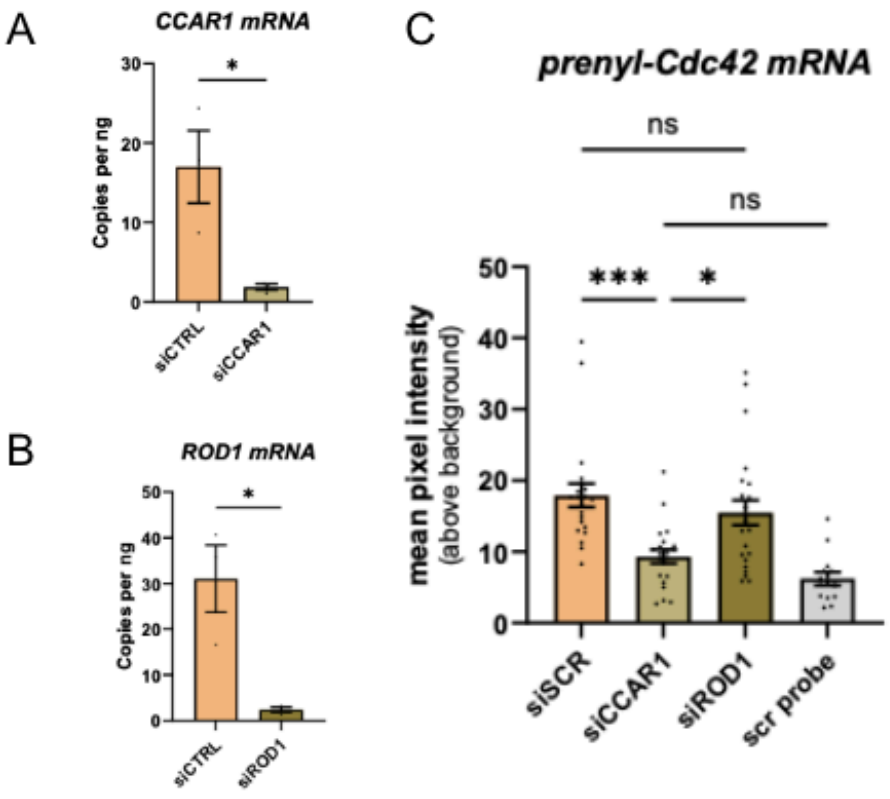

Figure 4.6: Knockdown of CCAR1 blocks axonal localization of *prenyl-Cdc42* mRNA. (A) (B) siRNA knockdowns of CCAR1 and PTBP3 (ROD1) were successful. (C) Stellaris FISH quantification of signal pixel intensity for adult DRG neuron cultures transfected with eGFPmyr3'*prenyl-Cdc42*$^{764\text{-}800}$ and CCAR1, PTBP3, and SCR knockdowns. FISH/IF analyses show that CCAR1 knockdown is sufficient for decrease in eGFPmyr3'*prenyl-Cdc42*$^{764\text{-}800}$ localization. PTBP3 knockdown is not sufficient in decreasing eGFPmyr3'*prenyl-Cdc42*$^{764\text{-}800}$ localization. (**** $P \leq 0.001$, *** $P \leq 0.005$, ** $P \leq 0.01$, * $P \leq 0.05$).

5. Discussion

5.1 Summary of results, goals and big picture of experiment

The goal of this experiment was to identify the mechanism underlying selective axonal localization of *prenyl-Cdc42* mRNA. Briefly, my data indicate that *prenyl-Cdc42* mRNA localizes through nt 764-800 in its proximal 3'UTR. Both CCAR1 and PTBP3 bind to this motif, and the interaction with CCAR1 appears to be necessary for maintaining axonal levels of *prenyl-Cdc42* mRNA.

Proteins are known to be synthesized intra-axonally and can contribute axon growth following injury to periphery neurons. There are also thousands of mRNAs now known to localize into the axons. CDC42 is a protein that promotes growth at the growth cones in axons after damage to the neuron and *prenyl-Cdc42* mRNA localizes into axons. RNA sequence motifs, frquently located in 3'UTRs, are responsible for loalization with RBPs binding to these motifs to drive the axonal localization. The collective results from the experiments conducted here show that nt 764-800, which is the most proximal region of *prenyl-Cdc42* mRNA 3'UTR, is necessary and sufficient for axonal localization of the mRNA.

RNA/protein affinity analyses indicate that CCAR1 and PTBP3 bind to the 3'UTR localizing motif of *prenyl-Cdc42* mRNA. Moreover, depletion of CCAR1, but not PTBP3, indicate *prenyl-Cdc42* mRNA/CCAR1 interaction is needed for maintiaing axonal levels of *prenyl-Cdc42* mRNA. This could either be from transport of *prenyl-Cdc42* mRNA into axons via CCAR1 interaction or stabilization of *prenyl-Cdc42* mRNA by CCAR1 binding in axons. The function of the *prenyl-Cdc42* mRNA/PTBP3 interaction was not uncovered from our experiements. Also, it is not clear whether *prenyl-Cdc42* mRNA/MBNL1 interaction is valid as

the antibodies for MBNL1 gave spurious signals on immunoblotting. More data is required to make a conclusion on whether MBNL1 binds to *prenyl-Cdc42* mRNA and the function of that interaction, as well as the functional significance of the PTBP3 interaction.

CCAR1 plays a big role in cell cycle regulation and cellular apoptosis. CCAR1 is also a known RBP that can associate with other proteins and be transported to stress granules via microtubules (Kolobova et al., 2009). As for PTBP3, a recent published study showed that a related protein, PTPB1, which functions in sensation, injury response and axonal regeneration in adult neurons, localizes into axons and associates with mRNAs known to respond to injury in neurons (Alber et al., 2023). Also, PTBP1 levels markedly increase after axonal injury. However, this protein seems to have a function in mRNA storage, rather than assisting in their localization into axons (Alber et al., 2023).

These results taken together suggest the mechanism for axonal localization of *prenyl-Cdc42* mRNA, giving a better understanding of how to alter this mechanism to increase certain axonal responses to CDC42, and therefore increase axonal regeneration rate.

5.2 Limitations & troubleshooting

One issue that presented itself was during cloning. Initially the cDNA inserts were unable to ligate into the plasmid vector possibly due to the plasmid vector not cutting properly with the HindIII and EcoR1 restriction enzymes. To resolve this, a new vector, 5' CaMKlla-myr-EGFP 3' gamma-actin, was cut instead with enzymes Not1 and Xho1. With continued cloning issues, we hypothesized that the overhangs produced by the restriction enzymes were preventing ligation between the vector and the inserts. This was due to the lack of flanking nucleotides blocking restriction enzyme digest of insert, which left its ends blunt. To overcome this, the

vector was treated with Klenow (to fill in the 5' overhangs by covalent bounding of free deoxynucleotides to blunt ends), heat inactivation, Quick CIP (to dephosphorylate 5' ends and block recircularization of the vector), and Zymo Research's DNA cleanup kits (to remove inhibitors from nucleic acid solutions) (Zymo Reseach) to fill in the overhangs and purify the vector. Due to the dephosphorylation of the vector, T4 polynucleotide Kinase (New England Bio) was used to phosphorylate the ends of the inserts so they could ligate into the vector. Orientation of ligated vector and inserts were checked with targeted restriction enzyme digest and sequencing.

Another problem arose from blunting of the ends of the vector. This allowed the vector to easily ligate to itself without incorporation of the insert. This was detected by gel electrophoresis. To combat this issue, the amount of insert being used was increased and successful ligation of insert into the plasmid was consequently obtained.

The final problem that occurred was that the agarose gel was not able to validate the results, as the insertion piece was far too small to be resolved by electrophoresis. At first, the same restriction enzymes used to cut initially (Not1 and Xho1) were being used in this assessment step of successful cloning. However, the insert was too small to be recognized on the gel, so HindIII was used to cut a larger portion of the plasmid. Since there was only one cut sequence within the vector and a second in the inserts, the final products would be different sizes with and without incorporation of the inserts. Using this method, we were able to validate successful cloning of our vector.

5.3 Implications in the field

Nervous system injury can be permanent or difficult to recover from. Within the PNS, regeneration is possible, although the rate is slow. The sciatic nerve, the largest bundle of motor and sensory neurons in the PNS, is easily injured due to its size. Also due to its length, the injury of this nerve is difficult to recover from since most tissue dies before the nerve as time to reinnervate distal areas of the body.

The overall goal of this project was to gain insight into mechanisms that can potentially lead to better treatment options for individuals suffering from PNS damage, specifically sciatic nerve injury. Since sciatic nerve injury recovery can occur slowly, especially due to Schwann cell death and extracellular environment inhibitors, finding an intracellular solution to increasing regeneration rate is important. Knowledge of the mechanism of *prenyl-Cdc42* mRNA gives insight to how this protein may be regulated differently to increase regeneration growth in injured sciatic nerves. Before being able to alter levels of this protein, or of other proteins playing a role in its antagonism, agonism, or localization, it was important to identify what proteins bind to *prenyl-Cdc42* mRNA and how this mRNA localizes into the axon. These results will lend to future experimentation in continuing the search for better treatment options for sciatic nerve injury.

5.4 Future directions

Lending to the continuation of sciatic nerve injury recovery, future projects should focus on the alteration of known mRNA and protein mechanisms that affect axon growth. There are many other localizing RBPs that associate with *prenyl-Cdc42* mRNA. Although CCAR1 was identified to be one of *prenyl-Cdc42* mRNA's RBPs, there are more that exist, as it is known from research on other RNPs that there is always a complex of multiple proteins to localize

mRNAs into axons. There were also other proteins identified from the RAMS analysis as potential hits. MBNL1 also needs more research conducted on it to either accept it as one of *prenyl-Cdc42* mRNA's RBPs or rule it out. Gaining further information on the mechanism for the axonal localization of *prenyl-Cdc42* mRNA will continue illuminate how to modify it to decrease regeneration time.

However, there is more that contributes to CDC42 effect on axon growth than simply localization. Stabilization and extrinsic factors also affect the CDC42 mechanism. There are many different proteins that interact with CDC42, and on an even larger scale there are whole pathways that consists of many proteins that influence axon growth and regeneration after injury. Future experiments should be conducted with the goal in mind of uncovering these pathways and in what ways these can be altered to enhance regeneration of axons. For example, it is known that the RBP KHSRP is an antagonist of CDC42 and many other axonally localized proteins, decreasing the stability of their mRNAs. Thus, targeting RBPs may provide strategies for promoting regeneration of injured nerves and possibly injured brain and spinal cord.

Finally, a post-doctoral fellow in Twiss lab has conducted research on various extrinsic factors that increase vs. decrease axon growth and converge on regulation of axonal Prenyl-CDC42. For example, preliminary research has been conducted on the effects of neurotrophins on axon growth. Neurotrophins are important for development, especially by helping to guide axon growth toward correct innervation sites. It has been hypothesized that neurotrophins carry this function out by working through CDC42's ability to increase axon growth. Further experimentation in necessary to investigate this possibility, as well as with other external cues that may lead to over- or under-expression of CDC42.

6. References

Ahimsadasan, N., Reddy, V., Khan Suheb, M. Z., & Kumar, A. (2024). Neuroanatomy, Dorsal Root Ganglion. In *StatPearls*. StatPearls Publishing. http://www.ncbi.nlm.nih.gov/books/NBK532291/

Alber, S., Di Matteo, P., Zdradzinski, M. D., Dalla Costa, I., Medzihradszky, K. F., Kawaguchi, R., Di Pizio, A., Freund, P., Panayotis, N., Marvaldi, L., Doron-Mandel, E., Okladnikov, N., Rishal, I., Nevo, R., Coppola, G., Lee, S. J., Sahoo, P. K., Burlingame, A. L., Twiss, J. L., & Fainzilber, M. (2023). PTBP1 regulates injury responses and sensory pathways in adult peripheral neurons. Science advances, 9(30), eadi0286. https://doi.org/10.1126/sciadv.adi0286

Bhatheja, K., & Field, J. (2006). Schwann cells: Origins and role in axonal maintenance and regeneration. *The International Journal of Biochemistry & Cell Biology*, *38*(12), 1995–1999. https://doi.org/10.1016/j.biocel.2006.05.007

Chapman, E. R. (2008). How Does Synaptotagmin Trigger Neurotransmitter Release? *Annual Review of Biochemistry*, *77*(1), 615–641. https://doi.org/10.1146/annurev.biochem.77.062005.101135

Chavarria, A., & Alcocer-Varela, J. (2004). Is damage in central nervous system due to inflammation? *Autoimmunity Reviews*, *3*(4), 251–260. https://doi.org/10.1016/j.autrev.2003.09.006

Chen, W., Datzkiw, D., & Rudnicki, M. A. (2020). Satellite cells in ageing: Use it or lose it. *Open Biology*, *10*(5), 200048. https://doi.org/10.1098/rsob.200048

Cramer, P., Armache, K.-J., Baumli, S., Benkert, S., Brueckner, F., Buchen, C., Damsma, G. E., Dengl, S., Geiger, S. R., Jasiak, A. J., Jawhari, A., Jennebach, S., Kamenski, T.,

Kettenberger, H., Kuhn, C.-D., Lehmann, E., Leike, K., Sydow, J. F., & Vannini, A. (2008). Structure of Eukaryotic RNA Polymerases. *Annual Review of Biophysics*, *37*(1), 337–352. https://doi.org/10.1146/annurev.biophys.37.032807.130008

Dalla Costa, I., Buchanan, C. N., Zdradzinski, M. D., Sahoo, P. K., Smith, T. P., Thames, E., Kar, A. N., & Twiss, J. L. (2021). The functional organization of axonal mRNA transport and translation. *Nature Reviews Neuroscience*, *22*(2), Article 2. https://doi.org/10.1038/s41583-020-00407-7

David, S., & Aguayo, A. J. (1981). Axonal Elongation into Peripheral Nervous System ``Bridges'' after Central Nervous System Injury in Adult Rats. *Science*, *214*(4523), 931–933.

Etienne-Manneville, S., & Hall, A. (2002). Rho GTPases in cell biology. *Nature*, *420*(6916), 629–635. https://doi.org/10.1038/nature01148

Filbin, M. T. (2003). Myelin-associated inhibitors of axonal regeneration in the adult mammalian CNS. *Nature Reviews. Neuroscience*, *4*(9), 703–713. https://doi.org/10.1038/nrn1195

Gomes, C., Merianda, T. T., Lee, S. J., Yoo, S., & Twiss, J. L. (2014). Molecular Determinants of the Axonal mRNA Transcriptome. *Developmental Neurobiology*, *74*(3), 218–232. https://doi.org/10.1002/dneu.22123

Höke, A. (2006). Mechanisms of Disease: What factors limit the success of peripheral nerve regeneration in humans? *Nature Clinical Practice Neurology*, *2*(8), 448–454. https://doi.org/10.1038/ncpneuro0262

Höke, A., & Brushart, T. (2010). Introduction to special issue: Challenges and opportunities for regeneration in the peripheral nervous system. *Experimental Neurology*, *223*(1), 1–4. https://doi.org/10.1016/j.expneurol.2009.12.001

Kalinski, A. L., Yoon, C., Huffman, L. D., Duncker, P. C., Kohen, R., Passino, R., Hafner, H., Johnson, C., Kawaguchi, R., Carbajal, K. S., Jara, J. S., Hollis, E., Geschwind, D. H., Segal, B. M., & Giger, R. J. (2020). Analysis of the immune response to sciatic nerve injury identifies efferocytosis as a key mechanism of nerve debridement. *eLife*, *9*, e60223. https://doi.org/10.7554/eLife.60223

Kalpachidou, T., Spiecker, L., Kress, M., & Quarta, S. (2019). Rho GTPases in the Physiology and Pathophysiology of Peripheral Sensory Neurons. *Cells*, *8*(6), 591. https://doi.org/10.3390/cells8060591

Kim, M. D., Kolodziej, P., & Chiba, A. (2002). Growth Cone Pathfinding and Filopodial Dynamics Are Mediated Separately by Cdc42 Activation. *Journal of Neuroscience*, *22*(5), 1794–1806. https://doi.org/10.1523/JNEUROSCI.22-05-01794.2002

Kolobova, E., Efimov, A., Kaverina, I., Rishi, A. K., Schrader, J. W., Ham, A. J., Larocca, M. C., & Goldenring, J. R. (2009). Microtubule-dependent association of AKAP350A and CCAR1 with RNA stress granules. Experimental cell research, 315(3), 542–555. https://doi.org/10.1016/j.yexcr.2008.11.011

Lee, S. J., Kar, A. N., Zdradzinski, M. D., Patel, P., Sahoo, P. K., Kawaguchi, R., Aguilar, B. J., Lantz, K. D., McCain, C. R., Coppola, G., Lu, Q., & Twiss, J. L. (2018). *Selective axonal translation of prenylated Cdc42 mRNA isoform supports axon growth* [Preprint]. Neuroscience. https://doi.org/10.1101/366369

Lee, S. J., Zdradzinski, M. D., Sahoo, P. K., Kar, A. N., Patel, P., Kawaguchi, R., Aguilar, B. J., Lantz, K. D., McCain, C. R., Coppola, G., Lu, Q., & Twiss, J. L. (2021). Selective axonal translation of the mRNA isoform encoding prenylated Cdc42 supports axon growth. *Journal of Cell Science*, *134*(7), jcs251967. https://doi.org/10.1242/jcs.251967

Lee, Y., & Rio, D. C. (2015). Mechanisms and Regulation of Alternative Pre-mRNA Splicing. *Annual Review of Biochemistry*, *84*(1), 291–323. https://doi.org/10.1146/annurev-biochem-060614-034316

Leppek, K., Das, R., & Barna, M. (2018). Functional 5′ UTR mRNA structures in eukaryotic translation regulation and how to find them. *Nature Reviews. Molecular Cell Biology*, *19*(3), 158–174. https://doi.org/10.1038/nrm.2017.103

Li, L., Yu, J., & Ji, S.-J. (2021). Axonal mRNA localization and translation: Local events with broad roles. *Cellular and Molecular Life Sciences*, *78*(23), 7379–7395. https://doi.org/10.1007/s00018-021-03995-4

Lytle, J. R., Yario, T. A., & Steitz, J. A. (2007). Target mRNAs are repressed as efficiently by microRNA-binding sites in the 5′ UTR as in the 3′ UTR. *Proceedings of the National Academy of Sciences*, *104*(23), 9667–9672. https://doi.org/10.1073/pnas.0703820104

Minc, N., Bratman, S. V., Basu, R., & Chang, F. (2009). Establishing New Sites of Polarization by Microtubules. *Current Biology*, *19*(2), 83–94. https://doi.org/10.1016/j.cub.2008.12.008

Olguin, S. L., Patel, P., Buchanan, C. N., Dell'Orco, M., Gardiner, A. S., Cole, R., Vaughn, L. S., Sundararajan, A., Mudge, J., Allan, A. M., Ortinski, P., Brigman, J. L., Twiss, J. L., & Perrone-Bizzozero, N. I. (2022). KHSRP loss increases neuronal growth and synaptic transmission and alters memory consolidation through RNA stabilization. *Communications Biology*, *5*(1), Article 1. https://doi.org/10.1038/s42003-022-03594-4

Patel, P., Buchanan, C. N., Zdradzinski, M. D., Sahoo, P. K., Kar, A. N., Lee, S. J., Vaughn, L. S., Urisman, A., Oses-Prieto, J., Dell'Orco, M., Cassidy, D. E., Costa, I. D., Miller, S., Thames, E., Smith, T. P., Burlingame, A. L., Perrone-Bizzozero, N., & Twiss, J. L. (2022).

Intra-axonal translation of Khsrp mRNA slows axon regeneration by destabilizing localized mRNAs. *Nucleic Acids Research*, *50*(10), 5772–5792. https://doi.org/10.1093/nar/gkac337

Polleux, F., & Snider, W. (2010). Initiating and Growing an Axon. *Cold Spring Harbor Perspectives in Biology*, *2*(4), a001925–a001925. https://doi.org/10.1101/cshperspect.a001925

Sievers, F., Wilm, A., Dineen, D., Gibson, T. J., Karplus, K., Li, W., Lopez, R., McWilliam, H., Remmert, M., Söding, J., Thompson, J. D., & Higgins, D. G. (2011). Fast, scalable generation of high-quality protein multiple sequence alignments using Clustal Omega. *Molecular Systems Biology*, *7*, 539. https://doi.org/10.1038/msb.2011.75

Silver, J., & Miller, J. H. (2004). Regeneration beyond the glial scar. *Nature Reviews Neuroscience*, *5*(2), Article 2. https://doi.org/10.1038/nrn1326

Taylor, A. M., Wu, J., Tai, H.-C., & Schuman, E. M. (2013). Axonal Translation of β-Catenin Regulates Synaptic Vesicle Dynamics. *The Journal of Neuroscience*, *33*(13), 5584–5589. https://doi.org/10.1523/JNEUROSCI.2944-12.2013

Terenzio, M., Koley, S., Samra, N., Rishal, I., Zhao, Q., Sahoo, P. K., Urisman, A., Marvaldi, L., Oses-Prieto, J. A., Forester, C., Gomes, C., Kalinski, A. L., Di Pizio, A., Doron-Mandel, E., Perry, R. B.-T., Koppel, I., Twiss, J. L., Burlingame, A. L., & Fainzilber, M. (2018). Locally translated mTOR controls axonal local translation in nerve injury. *Science (New York, N.Y.)*, *359*(6382), 1416–1421. https://doi.org/10.1126/science.aan1053

Turkman, A., Thanaraaj, V., Soleimani-Nouri, P., Harb, E., & Thakkar, M. (2023). Outcomes of Sciatic Nerve Injury Repairs: A Systematic Review. *Eplasty*, *23*, e42.

Twiss, J. L., Smith, D. S., Chang, B., & Shooter, E. M. (2000). Translational control of ribosomal protein L4 mRNA is required for rapid neurite regeneration. *Neurobiology of Disease*, *7*(4), 416–428. https://doi.org/10.1006/nbdi.2000.0293

Wang, W., van Niekerk, E., Willis, D. E., & Twiss, J. L. (2007). RNA transport and localized protein synthesis in neurological disorders and neural repair. *Developmental Neurobiology*, *67*(9), 1166–1182. https://doi.org/10.1002/dneu.20511

Xie, J., Zhuang, Z., Gou, S., Zhang, Q., Wang, X., Lan, T., Lian, M., Li, N., Liang, Y., Ouyang, Z., Ye, Y., Wu, H., Lai, L., & Wang, K. (2023). Precise genome editing of the Kozak sequence enables bidirectional and quantitative modulation of protein translation to anticipated levels without affecting transcription. Nucleic acids research, 51(18), 10075–10093. https://doi.org/10.1093/nar/gkad687

Zdradzinski, M. (2023). Molecular Mediators of Axonal Transport and Local Translation Of CDC42, RHOA Molecular Mediators of Axonal Transport and Local Translation of and Calreticulin mRNAs and Their Implications for Axon Growth and Regeneration. *Theses and Dissertations*. https://scholarcommons.sc.edu/etd/7404